La Nina and El Nino—induced variabilities of ozone in the tropical lower atmosphere during 1970–2001

J. R. Ziemke[1,2] and S. Chandra[2]

[1]   This study provides the first evidence from several decades of satellite measurements that both La Nina and El Nino events have a comparable and dramatic impact in altering the interannual variability and distribution of tropospheric ozone in the tropics. Measurements of tropospheric ozone were combined from several total ozone mapping spectrometer (TOMS) and backscatter ultraviolet (BUV) satellite instruments to establish long time series in the tropics extending from April 1970 through December 2001. The changes in tropospheric column ozone (TCO) for both La Nina and El Nino are sizeable when compared to local values which average from less than 15 Dobson Units (DU) up to 25 DU over the year. It is suggested that interannual changes in TCO from combined La Nina and El Nino are the dominant source of decadal variability in the tropics.   INDEX TERMS: 0365 Atmospheric Composition and Structure: Troposphere—composition and chemistry; 0368 Atmospheric Composition and Structure: Troposphere—constituent transport and chemistry; 1610 Global Change: Atmosphere (0315, 0325); 3339 Meteorology and Atmospheric Dynamics: Ocean/atmosphere interactions (0312, 4504); 3374 Meteorology and Atmospheric Dynamics: Tropical meteorology; KEYWORDS: El Nino, La Nina, Troposphere, Ozone, TOMS, BUV.
Citation: Ziemke, J. R., and S. Chandra, La Nina and El Nino—induced variabilities of ozone in the tropical lower atmosphere during 1970–2001, Geophys. Res. Lett., 30(3), 1142, doi:10.1029/2002GL016387, 2003.

1.   Introduction

[2]   It is well known that El Nino and La Nina events originate from planetary-scale changes in ocean temperature over the tropical Pacific and are associated with intense dynamical interactions between atmosphere and ocean [e.g., *Philander*, 1990, and references therein]. During El Nino the warm ocean temperature in the western Pacific shifts gradually from west of the dateline eastward into the eastern Pacific, eventually to South America. These eastward shifts in sea surface temperature associated with El Nino may extend for more than a year. The warm surface temperatures are accompanied by enhanced convection and the eastward shift coincides with dramatic changes in tropospheric wind distributions in the tropics. During La Nina a generally opposite condition occurs with warm oceanic temperatures west of the dateline which produces enhanced convection in the western Pacific. East of the dateline the La Nina conditions induce colder than normal sea surface temperatures and lower than normal tropical convection events.

[3]   The studies by *Chandra et al.* [1998, 2002], *Ziemke et al.* [1998], *Langford et al.* [1998], *Ziemke and Chandra* [1999], *Thompson et al.* [2001], and *Newchurch et al.* [2001] all indicated large interannual variabilities in observed tropospheric ozone associated with El Nino events. The largest detected changes (increases) in tropospheric column ozone (TCO) over the time period from January 1979 through 2000 occurred during September–November 1997 over Indonesia in the western Pacific with up to 25 Dobson Unit (DU) increases from average levels. Ozonesonde measurements at Watukosek (8°S, 113°E) in Indonesia also showed marked increases during these months of more than 100% normal levels [*Fujiwara et al.*, 1999, 2000]. These increases in ozone in late 1997 were examined in detail by *Sudo and Takahashi* [2001] and *Chandra et al.* [2002] which both incorporated observational data with a 3D photochemical transport model. Around half of the large increases in TCO over Indonesia during September–November 1997 were attributed to biomass burning. The remaining increases over Indonesia (and decreases over the eastern Pacific) were attributed to large-scale dynamical changes associated with El Nino. Low (high) surface pressure is associated with lower-tropospheric convergence (divergence) which produces reductions (increases) in TCO from enhanced (suppressed) upwelling [*Chandra et al.*, 1998]. Both the Harvard GEOS-CHEM [*Chandra et al.*, 2002] and University of Tokyo [*Sudo and Takahashi*, 2001] 3D photochemical transport models were able to quantify these changes in TCO associated with the 1997–1998 El Nino event.

[4]   In this investigation we employ satellite measurements of tropospheric ozone for the time period 1970–2001 in the tropics by combining TCO measurements from the Convective Cloud Differential (CCD) [*Ziemke et al.*, 1998] and the Simplified Tropospheric Ozone Residual (STOR) [*Ziemke and Chandra*, 1999] algorithms. An overview of the data used is described in section 2, followed by La Nina and El Nino time series comparisons of TCO and surface pressure in section 3, spatial patterns associated with La Nina and El Nino in section 4, and then a final summary of results.

2.   Tropospheric Column Ozone in the Tropics for 1970–2001

[5]   TCO for April 1970–December 2001 was derived from combined CCD and STOR methods. The CCD method utilizes high reflectivity (R > 0.9) scenes in the Pacific and low reflectivity (R < 0.2) scenes of total ozone to determine TCO. The STOR method uses only total column ozone measurements to determine TCO. In addition, the STOR method makes use of the weak variability of

---

[1]UMBC Goddard Earth Sciences and Technology (GEST) Center, Baltimore, Maryland, USA.
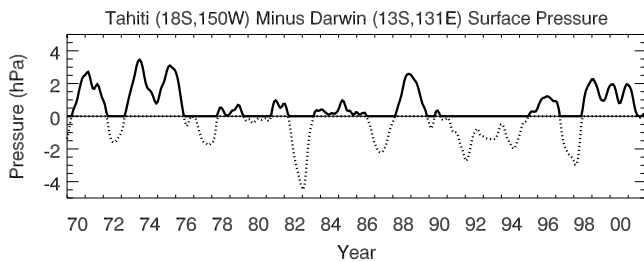[2]NASA Goddard Space Flight Center, Greenbelt, Maryland, USA.

Figure 1. Time series of the "Southern Oscillation Index" (SOI) for 1970–2001. Positive values (solid) correspond to La Nina conditions. Negative values (dotted) correspond to El Nino conditions. The proxies *LaNina*(*t*) and *ElNino*(*t*) in section 4 are respectively the solid and dotted curves in this figure. The SOI time series was smoothed with a lowpass filter having half-amplitude response at 12-month period.

TCO near the dateline to calculate stratospheric column ozone (SCO) over the region as a function of latitude and time. The STOR algorithm (as with the CCD algorithm) further assumes that SCO is predominantly zonally invariant in the tropics. Zonal homogeneity in SCO in the tropics has been demonstrated from many years of satellite and ground-based ozonesonde measurements [*Fishman and Larsen*, 1987; *Shiotani and Hasebe*, 1994; *Ziemke et al.*, 1996, 1998; *Thompson et al.*, 2002]. As discussed by *Ziemke et al.* [1998], the assumption of zonal invariance is limited mostly to lower tropical latitudes up to around ±15°. Local measurements of TCO from the CCD method are determined at each gridpoint by subtracting low reflectivity (R < 0.2) clear-sky total column ozone from Pacific SCO. Similarly, local measurements of TCO from the STOR method are derived at each gridpoint by subtracting Pacific SCO values from local measurements of total column ozone. As noted by *Ziemke and Chandra* [1999], local RMS differences between coincident CCD and STOR TCO generally vary from 2 to 4 DU.

[6] Measurements of total column ozone from several total ozone mapping spectrometer (TOMS) and backscatter ultraviolet (BUV) instruments were combined to generate monthly mean TCO in the tropics for the time period April 1970 through December 2001. TCO data were gridded at 5° × 5° resolution centered at longitudes −177.5°, −172.5°, …,177.5°, and latitudes −12.5°, −7.5°, …, 12.5°. Total ozone measurements used to generate TCO include Nimbus 4 BUV version 5 for April 1970–June 1976, Nimbus 7 (N7) TOMS version 7 for January 1979–April 1993, and Earth Probe (EP) TOMS version 7 for August 1996–December 2001). In addition, total ozone measurements from NASA "merged" total ozone data [Richard Stolarski, personal communication, 2002] were included to bridge the gap of missing TOMS measurements for May 1993 through July 1996. The merged ozone data for this time period include (version 6) measurements from NOAA 9 and NOAA 11 solar BUV (SBUV) satellite instruments. Details regarding the NASA merged total ozone data are available at the web site http://hyperion.gsfc.nasa.gov/Data_services/merged. CCD TCO was used for the N7 and EP time periods. STOR TCO was used to fill remaining time periods (i.e., the BUV time period and gap between N7 and EP). We note that a 5 DU offset was subtracted from CCD TCO for the EP time period [*Ziemke and Chandra*, 1999]. This offset primarily affects

clear-sky scenes and has been corrected in TOMS version 8 data (to be released in year 2003) [P. K. Bhartia, personal communication, 2002].

3. La Nina and El Nino: Tropospheric Ozone and Surface Pressure Time Series

[7] Figure 1 shows the "Southern Oscillation Index" (SOI) for the time period 1970–2001. The SOI time series in Figure 1 was derived from deseasonalized monthly mean tropical Tahiti minus tropical Darwin surface pressure as an indicator of El Nino and La Nina events in the Pacific. The surface pressure data were obtained from the Joint Institute for the Study of the Atmosphere and the Oceans (JISAO). (The data are available at the web site http://tao.atmos. washington.edu/data_sets/.) Deseasonalization of time series was accomplished by first computing annual cycle monthly averages for 1970–2001 and then subtracting from respective monthly values in the 32-year time series. High surface pressure in the tropics is associated with suppressed convection, and low surface pressure is associated with enhanced convection. In Figure 1 La Nina and El Nino events are indicated by positive and negative pressure anomalies. La Nina (i.e., positive values in Figure 1) dominates most of the years from 1970 into 1976, 1988–1989, and late 1998 into year 2000. El Nino (negative values in Figure 1) is most pronounced in 1982–1983, 1987, 1991–1994, and 1997–1998. The most long-term persistence of either El Nino or La Nina occurred with the La Nina conditions dominating most of the early time record from 1970 into year 1976.

[8] El Nino events can generate large changes in TCO as previous studies have indicated. In this study we investigate whether or not La Nina events can generate changes in tropical TCO similar to El Nino. Figure 2 (top) shows deseasonalized surface pressure from Darwin (13°S, 131°E;
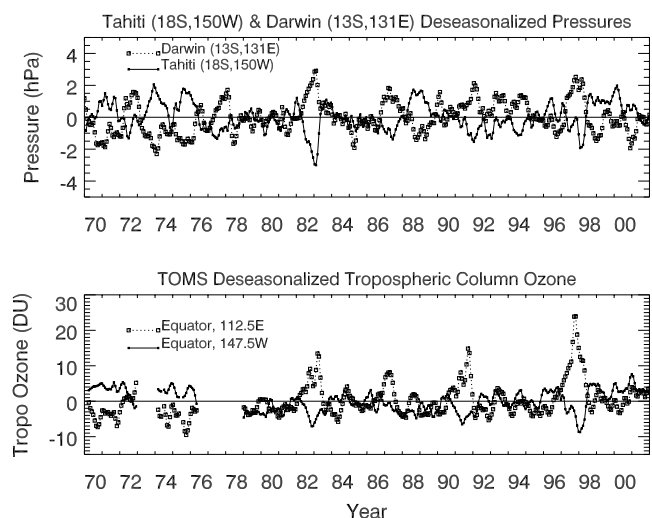

Figure 2. (top) Deseasonalized surface pressure time series from Darwin (13°S, 131°E; shown as boxes) in the western Pacific and Tahiti (18°S, 150°W; solid) in the eastern Pacific for years 1970–2001. (bottom) Deseasonalized CCD/STOR TCO time series along the Equator in the western Pacific (112.5°E) and eastern Pacific (147.5°W). All time series were smoothed with a 3-month running average.
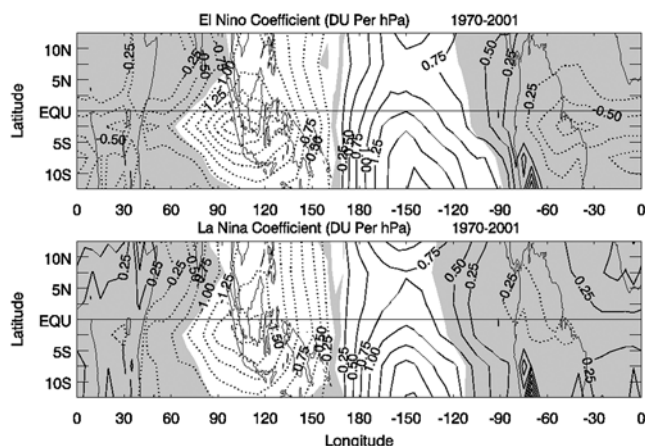
Figure 3. Annual mean regression coefficients in the tropics for El Nino (top) and La Nina (bottom) sources of TCO interannual variability derived from the regression analysis described by (1). Actual changes in TCO for El Nino are opposite in sign to coefficients shown. Shaded regions are not statistically significant at the 2σ level. Units are DU per hPa.

shown as boxes) in the western Pacific and Tahiti (18°S, 150°W; solid) in the eastern Pacific for years 1970–2001. Figure 2 (bottom) plots deseasonalized TCO along the Equator in the western Pacific (112.5°E) and eastern Pacific (147.5°W). The large increases in TCO over Indonesia in late 1997 caused by El Nino are evident in Figure 2 at 112.5°E which shows positive anomalies varying from around +5 DU up to +25 DU in 1997. Comparison with surface pressure and TCO in Figure 2 suggests that the interannual variability of TCO over the eastern and western Pacific is dominated by a combination of both El Nino and La Nina events. Surface pressure and TCO in Figure 2 are clearly positively correlated for either El Nino or La Nina both east and west of the dateline. The general conclusion from Figure 2 is that high surface pressure in the tropical Pacific coincides with increases in TCO and low surface pressure coincides with decreases in TCO.

[9] We note that the intense 1997–1998 El Nino event has been shown [e.g., Figure 4 of *Fujiwara et al.*, 2000] to reduce tropopause altitude over Indonesia by up to 1 km. This corresponds to around 15 hPa increase in tropopause pressure and about 1–2 DU reduction in TCO given 100–120 ppbv ozone in the upper troposphere in their figure. Although tropopause height may affect calculation of TCO it is small and has little direct impact in this study.

[10] The La Nina events encompassing 1970–1976, 1988–1989, and late 1998–2000 in Figure 2 all show reduced TCO in the western Pacific and increased TCO in the eastern Pacific. These La Nina episodes indicate east-west dipole changes about the dateline of around 5 DU for weak events and around 10 DU for strong events. In contrast the El Nino events in 1982–1983, 1987, 1991–1994, and 1997–1998 indicate an opposite dipole shift with around 5–10 DU east-west dipole differences for weak events and up to 15–25 DU differences for the strong events in 1982–1983 and 1997–1998. The time series in Figure 2 imply that El Nino and La Nina have opposite effects in altering the distribution of eastern and western Pacific TCO.

4. Spatial Pattern Distributions Associated With La Nina and El Nino

[11] A statistical linear regression approach is used to identify tropical pattern distributions relating to variabilities in TCO associated with La Nina and El Nino. Prior to regression analysis, TCO time series were deseasonalized and smoothed with a 3-month running average. The regression analysis of TCO data involved dynamical proxies of La Nina and El Nino as follows:

$$TCO(t) \ = A(t) \ ElNino(t) + B(t) \ LaNina(t) + R(t). \quad (1)$$

[12] In (1), t is the month index for January 1970–December 2001 (i.e., 384 months). $A(t)$ and $B(t)$ in (1) are seasonally-varying regression coefficients given by a constant plus 12-month and 6-month cosine and sine annual harmonic series [e.g., *Stolarski et al.*, 1991]. $ElNino(t)$ and $LaNina(t)$ proxies in (1) were derived from the SOI time series in Figure 1 from negative and positive anomalies, respectively. $R(t)$ in (1) is the residual (i.e., error) time series. The regression model ignores potential solar and quasi-biennial oscillation (QBO) forcings which appear to have much smaller amplitudes (∼2–3 DU) compared to El Nino [*Ziemke and Chandra*, 1999].

[13] Results of the regression analysis from (1) are shown in Figure 3 which prescribes annual mean regression coefficients in the tropics for both El Nino (top) and La Nina (bottom). Shaded regions in Figure 3 are not statistically significant at the 2σ level. The top contour plot in Figure 3 shows El Nino coefficients and indicates that the most intense El Nino signals occur in the western Pacific over Indonesia, and (of opposite sign) in the eastern Pacific. Because El Nino is associated with negative values in SOI, the negative coefficient values in the western Pacific in Figure 3 (top) correspond to positive changes in TCO, and positive coefficient values in the eastern Pacific correspond to negative changes in TCO. The regression coefficient distributions in Figure 3 for La Nina (bottom) show similar spatial patterns and amplitudes as El Nino which include a Pacific dipole structure about the dateline. A perhaps clearer construct of spatial patterns is to show projected amplitudes
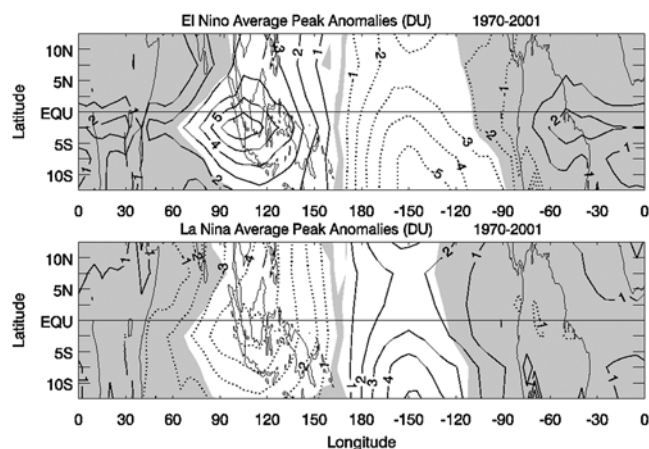

Figure 4. Average peak changes (DU) in TCO caused by El Nino (top) and La Nina (bottom) from the 32-year regression analysis. Shown are projected amplitudes (see section 4). Shaded regions are not statistically significant at the 2σ level.

(Figure 4). In this figure the coefficients from Figure 3 were multiplied by average peak values of *ElNino(t)* and *LaNina(t)* in Figure 1 (−3.1 hPa and 2.9 hPa, respectively) for the most robust cases (i.e., 3 major La Nina events, 4 major El Nino events). The main result from Figure 4 is that average peak changes in TCO during La Nina appear to show similar column amounts as El Nino but reversed in sign. Both La Nina and El Nino show east-west dipole differences averaging around 6−10 DU over latitude with marginally larger dipole differences for El Nino.

5. Summary

[14] This study has shown that both La Nina and El Nino events during the time period extending from 1970 through 2001 have had a significant effect in altering the distribution of tropical TCO on interannual time scales. The largest changes in TCO for both La Nina and El Nino events are centered over Indonesia in the equatorial western Pacific and spread out with opposite sign over the eastern Pacific. The analyses of 32 years of TCO data indicates that La Nina and El Nino have nearly opposite spatial patterns in TCO in the low-latitude tropics. Comparison with observed surface pressure for the 32-year time record shows significant correlation with TCO for both La Nina and El Nino events. That is, for either event increases (decreases) in pressure coincide closely with increases (decreases) in TCO both east and west of the dateline.

[15] El Nino events produce enhanced convection over the eastern Pacific and suppressed convection in the western Pacific. Generally opposite conditions prevail during La Nina. During El Nino, TCO is enhanced over the western Pacific and reduced over the eastern Pacific because of planetary-scale shifts in sea-surface temperature and convection. The analyses in this study suggest that El Nino produces an east-west dipole difference in TCO over the Pacific ranging from about 5−10 DU for weak events and up to 15−25 DU for strong events. La Nina events indicate a dipole in TCO about the dateline which is reversed from that of El Nino with weak events producing around 5 DU and strong events producing up to 10 DU dipole differences. For La Nina conditions in the tropics, TCO is reduced over the western Pacific and enhanced over the eastern Pacific. La Nina indicates nearly opposite spatial distributions in TCO in the tropics compared to El Nino.

[16] In years not affected by significant El Nino or La Nina occurrences, TCO over the broad eastern and western Pacific averages over the year from less than 15 DU up to around 25 DU. The large interannual anomalies in tropical TCO caused by combined El Nino and La Nina events appear to be the dominant source of decadal variability in the tropics.

References

Chandra, S., J. R. Ziemke, W. Min, and W. G. Read, Effects of 1997–1998 El Nino on tropospheric ozone and water vapor, *Geophys. Res. Lett.*, 25, 3867–3870, 1998.

Chandra, S., J. R. Ziemke, P. K. Bhartia, and R. V. Martin, Tropical tropospheric ozone: Implications for dynamics and biomass burning, *J. Geophys. Res.*, 4188, doi:10.1029/2001JD000447, 2002.

Fishman, J., and J. C. Larsen, Distribution of total ozone and stratospheric ozone in the tropics: Implications for the distribution of tropospheric ozone, *J. Geophys. Res.*, 92, 6627–6634, 1987.

Fujiwara, M., K. Kita, S. Kawakami, T. Ogawa, N. Komala, S. Saraspriya, and A. Suripto, Tropospheric ozone enhancements during the Indonesian forest fire events in 1994 and 1997 as revealed by ground-based observations, *Geophys. Res. Lett.*, 26, 2417–2420, 1999.

Fujiwara, M., K. Kita, T. Ogawa, S. Kawakami, T. Sano, N. Komala, S. Saraspriya, and A. Suripto, Seasonal variation of tropospheric ozone in Indonesia revealed by 5-year ground-based observations, *J. Geophys. Res.*, 105, 1879–1888, 2000.

Langford, A. O., T. J. O'Leary, C. D. Masters, K. C. Aikin, and M. H. Proffitt, Modulation of middle and upper tropospheric ozone at Northern midlatitudes by the El Nino/Southern Oscillation, *Geophys. Res. Lett.*, 25, 2667–2670, 1998.

Newchurch, M. J., X. Liu, and J. H. Kim, Lower-Tropospheric Ozone (LTO) derived from TOMS near mountainous regions, *J. Geophys. Res.*, 106, 20,403–20,412, 2001.

Philander, S. G. H., *El Nino, La Nina and the Southern Oscillation*, 289 pp., Academic, San Diego, Calif., 1990.

Shiotani, M., and F. Hasebe, Stratospheric ozone variations in the equatorial region as seen in Stratospheric Aerosol and Gas Experiment data, *J. Geophys. Res.*, 99, 14,575–14,584, 1994.

Stolarski, R. S., P. Bloomfield, R. D. McPeters, and J. R. Herman, Total ozone trends deduced from Nimbus 7 TOMS data, *Geophys. Res. Lett.*, 18, 1015–1018, 1991.

Sudo, K., and M. Takahashi, Simulation of tropospheric ozone changes during 1997–1998 El Nino: Meteorological impact on tropospheric photochemistry, *Geophys. Res. Lett.*, 23, 4091–4094, 2001.

Thompson, A. M., J. C. Witte, R. D. Hudson, H. Guo, J. R. Herman, and M. Fujiwara, Tropical tropospheric ozone and biomass burning, *Science*, 291, 2128–2132, 2001.

Thompson, A. M., et al., The 1998–2000 Southern Hemisphere Additional Ozonesondes (SHADOZ) tropical ozone climatology, 2, Tropospheric variability and the zonal wave-one, *J. Geophys. Res.*, 107, doi:1029/2002JD002241, 2002.

Ziemke, J. R., and S. Chandra, Seasonal and interannual variabilities in tropical tropospheric ozone, *J. Geophys. Res.*, 104, 21,425–21,442, 1999.

Ziemke, J. R., S. Chandra, A. M. Thompson, and D. P. McNamara, Zonal asymmetries in southern hemisphere column ozone: Implications of biomass burning, *J. Geophys. Res.*, 101, 14,421–14,427, 1996.

Ziemke, J. R., S. Chandra, and P. K. Bhartia, Two new methods for deriving tropospheric column ozone from TOMS measurements: The assimilated UARS MLS/HALOE and convective-cloud differential techniques, *J. Geophys. Res.*, 103, 22,115–22,127, 1998.

———————————
S. Chandra, Code 916, Chemistry and Dynamics Branch, NASA Goddard Space Flight Center, Greenbelt, MD 20771, USA.
J. R. Ziemke, Code 916, Chemistry and Dynamics Branch, NASA Goddard Space Flight Center, Greenbelt, MD 20771, USA. (ziemke@chescat.gsfc.nasa.gov)